Detection of giant muon families at the underground scintillation telescope of the Baksan Neutrino Observatory

V. N. Bakatanov, S. N. Boziev, Yu. F. Novosel'tsev, M. V. Novosel'tseva, and A. E. Chudakov

Institute of Nuclear Research, Russian Academy of Sciences, 117334, Moscow, Russia

(Submitted 30 July 1992)
Pis'ma Zh. Eksp. Teor. Fiz. **56**, No. 5, 237–241 (10 September 1992)

The detection method is discussed. Data from the detection of families with a high muon multiplicity ($E_\mu \geqslant 220$ GeV) over 31 648 h have been analyzed. The results are discussed.

The method. As was first shown in Ref. 1, the muon groups of extensive air showers constitute a source of information on the chemical composition of the primary cosmic rays. The method for detecting groups in the underground installations presently in operation is based on the selection of parallel particle trajectories which penetrate through the apparatus simultaneously. There are two methodological difficulties in such experiments. These difficulties affect the accuracy with which the muon multiplicity is determined and thus the reliability of the ultimate result. The first is the problem of locating the axis of the extensive air shower. The second is the problem of determining the multiplicity in cases in which the density of muons being detected is relatively high—so high that the trajectories of the muons incident on the apparatus cannot be distinguished at the prevailing spatial resolution. The problem of determining the position of the shower axis on the basis of muon groups was solved in Ref. 2 for a particular case, namely, the case in which high-energy cascades initiated by one of the muons of the group are detected (the term "muon families" was introduced in Refs. 3 and 4 for events in which the information on the multiplicity is supplemented by information on the energies of these muons). However, when so-called giant muon families, i.e., events with a high multiplicity of high-energy muons, are detected, a new opportunity for studying muon families opens up. A distinctive feature of this case is that a large energy evolution, representing a superposition of the energy losses of these muons, would be expected in the calorimeter. Since the density and energy of the muons increase toward the shower axis, a region of large energy evolution indicates the position of this axis. The magnitude of the energy evolution, ϵ, contains information on the multiplicity. The value of ϵ can be calculated by using the spatial-energy distribution of the muons of a family which was found in Ref. 5. For a primary energy $E_0 \gg E_\mu$ this function has the asymptotic behavior

$$f(r, \geq E_\mu) = C \exp(-r/r_0)^b,$$

where $r_0 = 0.95/(1 + 12.5E_\mu)^{0.92}$, $b = 0.43$, and C is a normalization factor. We have

$$\epsilon = n_\mu X \int_0^{r_e} r dr \int_{E_\mu + E_{min}}^{E_o} dE_\mu \frac{df(r, \geq E_\mu)}{dE_\mu} [a + \int_{E_{min}}^{E_\mu} W(E_\mu, E_k) E_k dE_k], \qquad (1)$$

where X is the absorber thickness, r_ϵ is the radius of the circle with the absorbed energy evolution, $a = 2$ MeV·cm^2/g, $E_{\min} = 10$ MeV, and $W(E_\mu, E_k)$ is the total number of particles with an energy E_k which are produced by a muon of energy E_μ in the course of the generation of e^+e^- pairs and δ-electrons, bremsstrahlung, and nuclear interactions. The behavior of W for these processes is taken from Refs. 6–9, respectively.

The number of muons in the family, n_μ, is found by comparing the measured energy evolution with that calculated from (1).

Experimental procedure. The telescope is a block (16.7×16.7×10.8 m) consisting of six outer and two inner (horizontal) layers. Each layer has about 400 detectors, overlapped to a thickness of 170 g/cm^2. A detector is a container (70×70×30 cm) with a liquid scintillator, which is monitored by an FÉU-49 photomultiplier. The information from the detector is transmitted over three channels: an anode channel, a pulse channel (from the twelfth dynode), and a logarithmic channel (from the fifth dynode). The anode signals are used in generating control signals. The pulse channel has an operation threshold, which is one-fourth of the most probable energy evolution (50 MeV) of a muon in a detector. The signal from the fifth dynode (with an operation threshold $\epsilon_5 = 0.5$ GeV) is used to measure large energy evolutions. The signal is converted into a pulse whose length t is proportional to the logarithm of the amplitude of the signal: $\epsilon_d = 1.23^{n_A - 1}\epsilon_5$, where $n_A = t/(10\ \mu\text{s})$.

The functional capabilities of the telescope in terms of the detection of giant families are augmented by two remote installations, at distances of 31 m (RI1) and 85 m (RI2) from the center of the telescope. These installations are plane arrays of scintillation detectors, each with an area $S = 9.8$ m^2.

The selection of events is triggered by the existence of a total energy evolution $\epsilon_\Sigma \geqslant 417$ GeV in the detectors which have operated. In the detectors for which a signal was generated from the pulse channel, while there was no signal from the amplitude channel, the energy evolution was assumed to be 75 MeV. Generally speaking, this assumption is valid only in the detection of cascades from individual muons. The energy evolution ϵ in (1) was thus determined from the signals from the amplitude channel of the detectors. Figure 1 shows the experimental field of points for the total number of detectors which have operated, m_{12}, and for the total number of detectors with a large energy evolution ($\epsilon_d \geqslant 0.5$ GeV; m_5) in the events selected by this triggering arrangement. This triggering arrangement is seen to result in the observation of two classes of events (which are represented by different symbols). These events refer to the cases, mentioned above, in which the large energy evolution in the telescope either is a consequence of the generation of high-energy cascades by individual muons or is observed as the result of the detection of giant muon families.

We assign nine events in this figure (shown by the crosses) to giant muon families. For them we observe the following obvious characteristics, which we will list without a detailed discussion. 1. A large number of detectors (m_{12}) operates with a relatively small energy evolution. 2. The cascade curve is not the curve characteristic of electromagnetic cascades. The cascade curve is reconstructed from the signals from the various planes of the telescope through which the shower axis passes. 3. There is no maximum in the spatial distribution of the observed energy evolutions from one

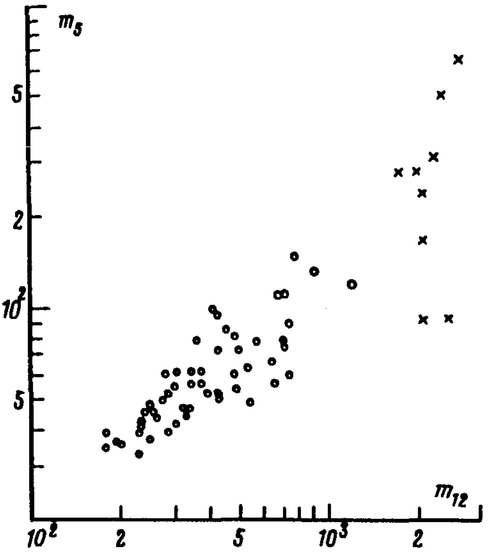

FIG. 1. Correlation in terms of the number of detectors, m_{12} and m_5, in events selected on the basis of the trigger condition $\epsilon_\Sigma \geqslant 417$ GeV.

layer, as would be characteristic of electromagnetic cascades. 4. Remote installations RI1 and RI2 operate. In three events of the nine, RI1 and RI2 operated; in five of the events, RI1 operated. In one case there was no signal from either RI1 or RI2. This situation turns out to agree with the most likely outcome for the given shower arrival direction and for the number of muons in the family determined from data on the energy evolution in the telescope. This analysis was carried out with the help of the spatial-energy distribution of the muons given above. In no case in which a cascade from a single muon was detected did RI1 and RI2 operate. 5. For four of the events, a coincidence was found with the Kover underground installation of the Baksan Neutrino Observatory, at a position 900 m from the telescope. In the five other cases, the coincidence circuit of the two installations was disconnected.

Figure 2 shows the muon multiplicities n_μ found for each of the nine events, converted to a vertical direction and to a threshold $E_\mu \geqslant 220$ GeV with the help of the

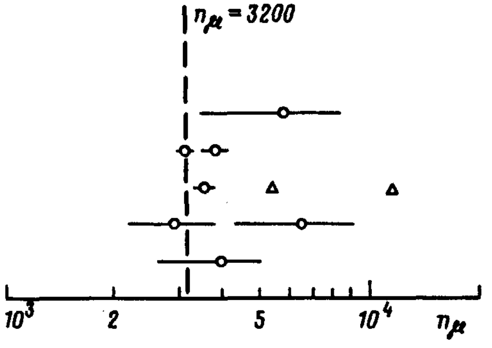

FIG. 2. Muon multiplicities in nine events. ●—Experimental errors and errors found from the signals from the various planes of the telescope; △—estimate of the multiplicity based on the density of muons at RI1 and RI2 and the given spatial-energy distribution.

expression derived in Ref. 10 for the average number of muons generated by primary nuclei:

$$\bar{n}_\mu(A, E_0, \geq E_\mu, \theta) = \frac{1.87\times 10^{-2} A x(\theta)}{E_\mu^{0.9+0.1\,\log E_\mu}} \left(\frac{E_0}{E_\mu}\right)^{0.78} \left(\frac{E_0}{E_0+E_\mu}\right)^{d}. \tag{2}$$

Here $d = E_\mu + 11.3/\log(10+0.5E_0)$; $x(\theta) = [1+36\ln(\cos\theta)]/\cos\theta$; A is the atomic weight; and E_0 is the energy per nucleon. The threshold multiplicity $n_\mu = 3200$ in Fig. 2 corresponds to a primary energy $E_0 \simeq 10^{17}$ eV.

To interpret the results of this experiment, we use the following approximation of the energy spectrum of the primary protons:

$$J(E_0)dE_0 = 1{,}5E_0^{-2{,}7}(1+E_0/E_{sc})^{-0.4}dE_0\ (\mathrm{cm}^2\cdot\mathrm{sr}\cdot\mathrm{s})/(\mathrm{GeV})^{-1},$$

where E_{sc} is the energy of the change in slope (sc). The spectra of the nuclei are similar to this spectrum, but the behavior of the slope change may depend on the atomic weight or atomic number Z of the nuclei. The data of Refs. 11–13 on extensive air showers with $E_0 \gtrsim 10^{17}$ eV agree with a change in slope at $E_c = 3\times 10^{15}$ eV/A or 3×10^{15} eV/Z.

Figure 3 shows the multiplicity distribution of events, found as

$$P(\geq n_\mu) = \sum_{i=n_\mu}^{\infty} \sum_{A} \frac{\rho_A}{\rho_1} \int_{E_\mu}^{\infty} B(i, \bar{n}_\mu, k) J(E_0) dE_0,$$

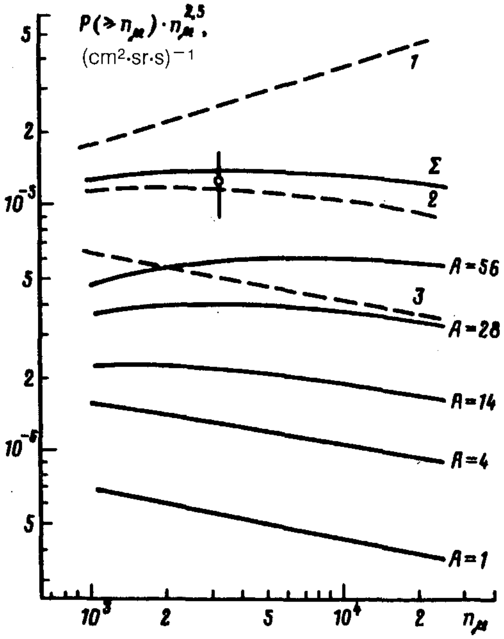

FIG. 3. Comparison of theoretical and experimental results for various versions of the change in slope. 1—No change in slope; $\Sigma - E_c = 3\times 10^{15}$ eV/A; 2—$E_c = 3\times 10^{15}$ eV/Z; 3—$E_c = 3\times 10^{15}$ eV. Here Σ is the sum of the distributions shown for the various components of the primary nuclei.

where $\bar{n}_\mu$ and B are the mean number of muons in (2) and the muon fluctuations according to a negative binomial distribution,[10] ρ_A is the relative abundance of nuclei at $E_0 \simeq 2$ GeV/A, $\rho_1 = 0.94$, $\rho_4 = 0.055$, $\rho_{14} = 0.0035$, $\rho_{28} = 0.0011$, and $\rho_{56} = 0.0003$. It follows from this comparison of experiment and theory that our results agree best with a change in slope in the primary spectrum with $E_{sc} \simeq 3 \times 10^{15}$ eV/A or $E_{sc} \simeq 3 \times 10^{15}$ eV/Z. This result offers support for the diffusion model for the propagation of cosmic rays in the local galaxy. It follows from Fig. 3 that the nuclei at $E_0 \gtrsim 10^{17}$ eV are not exclusively protons; the composition appears to be complex. These conclusions are preliminary. In order to find more-concrete results, it will be necessary to accumulate more experimental data and to analyze the data more accurately by statistical methods. It is also important to note that the method described here yields data on the chemical composition at $E_0 \gtrsim 10^{17}$ eV. This information supplements the data from extensive air showers at these energies.

[1] A. E. Chudakov, *Proc. of 16th ICRC, Vol. 10,* 1979, p. 192.
[2] V. N. Bakatanov *et al.*, Preprint P-0430, Institute of Nuclear Research, Academy of Sciences of the USSR, 1985.
[3] T. V. Danilova *et al.*, Preprint PTB-180, Univ. Bordeaux 1, 1988.
[4] R. P. Kokoulin and A. A. Petrukhin, Fiz. Elem. Chastits At. Yadra **21**, 774 (1990) [Sov. J. Part. Nucl. **21**, 332 (1990)].
[5] S. N. Boziev *et al.*, Preprint P-0630, Academy of Sciences of the USSR, 1989.
[6] R. P. Kokoulin and A. A. Petrukhin, *Proc. of 12th ICRC, Vol. 6,* 1971, p. 2436.
[7] S. Hayakawa, *Cosmic Ray Physics,* Wiley, New York, 1969.
[8] É. V. Bugaev *et al.*, *Cosmic Muons and Neutrinos, Vol. 15,* Nauka, Moscow, 1970.
[9] L. B. Bezrukov and E. V. Bugaev, *Proc. of 17th ICRC, Vol. 7,* 1981, p. 90.
[10] S. N. Boziev, Yad. Fiz. **52**, 500 (1990) [Sov. J. Nucl. Phys. **52**, 320 (1990)].
[11] M. Nagano *et al.*, J. Phys. G **18**, 423 (1992).
[12] M. N. Dyakonov *et al.*, *Proc. of 12th ICRC, Vol. 2,* 1991, p. 93.
[13] M. A. Lawrence *et al.*, J. Phys. G **17**, 733 (1991).

Translated by D. Parsons